THE JOURNAL OF PHYSICAL CHEMISTRY B

Article

pubs.acs.org/JPCB

Quantifying the Heterogeneous Dynamics of a Simulated Dipalmitoylphosphatidylcholine (DPPC) Membrane

Neha Shafique,[†,‡] Kiley E. Kennedy,[†,‡] Jack F. Douglas,[∥] and Francis W. Starr*[,†,§,‡]

[†]Department of Physics, [‡]Molecular Biophysics Program, and [§]Department of Molecular Biology and Biochemistry, Wesleyan University, Middletown, Connecticut 06459, United States

[∥]Materials Science and Engineering Division, National Institute of Standards and Technology, Gaithersburg, Maryland 20899, United States

ABSTRACT: Heterogeneity of dynamics plays a vital role in membrane function, but the methods for quantifying this heterogeneity are still being developed. Here we examine membrane dynamical heterogeneity via molecular simulations of a single-component dipalmitoylphosphatidylcholine (DPPC) lipid bilayer using the MARTINI force field. We draw upon well-established analysis methods developed in the study of glass-forming fluids and find significant changes in lipid dynamics between the fluid (L_α), and gel (L_β) phases. In particular, we distinguish two mobility groups in the more ordered L_β phase: (i) lipids that are transiently trapped by their neighbors and (ii) lipids with displacements on the scale of the intermolecular spacing. These distinct mobility groups spatially segregate, forming dynamic clusters that have characteristic time (1−2 μs) and length (1−10 nm) scales comparable to those of proteins and other biomolecules. We suggest that these dynamic clusters could couple to biomolecules within the membrane and thus may play a role in many membrane functions. In the equilibrium membrane, lipid molecules dynamically exchange between the mobility groups, and the resulting clusters are not associated with a thermodynamic phase separation. Dynamical clusters having similar characteristics arise in many other condensed phase materials, placing membranes in a broad class of materials with strong intermolecular interactions.

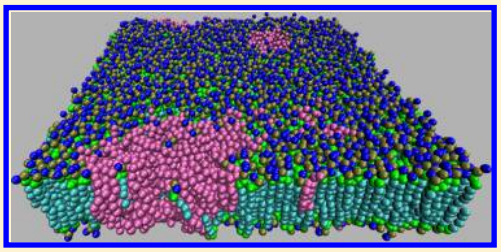

INTRODUCTION

Lipid membranes bustle with dynamic phenomena that underlie essential cellular processes such as transport and signaling. While the structural features of membranes have been carefully examined, their dynamical characteristics are less well understood.[1] It is increasingly appreciated that cell membranes have dynamic regions of associating molecules with properties that can differ significantly from their surroundings and that this "dynamic heterogeneity" is important for biological function.[2] Generally speaking, dynamic heterogeneity occurs in many condensed phase materials and is characterized by the existence of transient finite regions of either limited or enhanced mobility.[3,4] This phenomenon arises even in the absence of phase separation, and this form of dynamic heterogeneity should not be confused with composition or density fluctuations associated with phase separation. In lipid systems, the existence of such regions has been experimentally demonstrated by neutron scattering,[5−8] single-molecule tracking studies,[9,10] and rotational probe dynamics,[11] as well as molecular simulation.[12−18] The partitioning of membranes into laterally heterogeneous domains having different mobilities creates a tunable environment to modulate protein interactions and other cellular functions. Accordingly, the dynamical heterogeneity could give rise to intermittency of protein displacements in membranes,[19,20] and membrane fluidity shows a strong sensitivity to molecular additives (e.g., anesthetics, antibiotics, neurotransmitters, proteins) that influence molecular packing.[21−27] While there is widespread acknowledgment of the importance of these transient structures, a precise and quantifiable definition of heterogeneous dynamics in membranes remains a challenge.[1]

In the case of biological cell membranes, protein extraction, phase separation, and supramolecular assembly, all pose challenges to understanding membrane dynamics and their corresponding function. However, structural heterogeneity associated with phase separation, protein inclusions, or molecules bound to the membrane surface is *not* a prerequisite for observing dynamical heterogeneity; it has been demonstrated that even simple single-component lipid membranes have dynamics that are intrinsically heterogeneous.[12,13,15,18,28,29] Of course, structural heterogeneity in biological membranes can cause and/or complicate dynamic heterogeneity. Thus, we consider a "bottom-up" approach to the problem, where we begin by attempting to understand the fundamentals of cooperative dynamic motion within a model DPPC bilayer. Studying a single-component membrane allows us to identify effects intrinsic to lipid systems (rather than those that are a consequence of differing compositions and interactions) and is an important step toward a common framework that takes into account increasingly complex lipid

Received: March 22, 2016
Revised: May 24, 2016
Published: May 25, 2016

DOI: 10.1021/acs.jpcb.6b02982
J. Phys. Chem. B 2016, 120, 5172−5182

structures that effect dynamical heterogeneity within biological membranes. The first challenge that arises in this effort is how to quantitatively describe complex concerted molecular motions arising in these materials, even in the absence of compositional heterogeneity.

To address this challenge, we take advantage of the fact that dynamical heterogeneity is a ubiquitous and well-studied property in a broad class of dense, strongly interacting materials. Most notably, dynamical heterogeneity has been a topic of emphasis in glass-forming fluids,[3,4] and the theoretical tools to quantify collective motion in glass-forming fluids are fairly mature in their development.[30,31] Such fluids are characterized by strong intermolecular interactions relative to the effects of thermal energy, a situation that applies to the case of lipid membranes. While glass-forming fluids and lipid bilayers are clearly distinct material systems, strong intermolecular interactions could lead to a common tendency for clusters of relatively mobile molecules to form large scale transient domains and a tendency toward collective molecular rearrangement motion within these clusters. This relationship has not gone unnoticed in the literature, as previous studies have mentioned qualitative similarities between the observations of dynamic heterogeneity between lipid membranes and glass-forming fluids.[13,15,32−34] Recently, we directly applied methods developed in the context of glass formation to a simple coarse-grained lipid membrane model.[18] Given the simplicity of the model used,[35] validation of the previous findings for a more realistic lipid model is a prerequisite to the investigation of multicomponent membranes more relevant to living systems.

Accordingly, here we utilize the MARTINI force field[36] to simulate membranes comprised of dipalmitoylphosphatidylcholine (DPPC), probably the most studied lipid system, sometimes referred to as the "hydrogen atom of lipids".[37] The MARTINI model has been systematically parametrized to be quantitatively comparable to experimental studies, but allows for the simulation of much longer time and length scales than are feasible using traditional atomistic models. As we shall see, the characteristic length and times of heterogeneity in this system (order 10 nm and 1 μs) make it necessary to examine large systems over long timescales.

Our molecular dynamics simulations for a pure DPPC membrane demonstrate that intrinsic heterogeneity of the lipid motions occurs in the L_β gel phase, while the fluid L_α phase is characterized by simple Brownian dynamics. The difference is attributed to transient "caging" of lipids by their neighbors within the gel phase, similar to the dynamics seen in fluids approaching a glass transition. In the L_β phase, we demonstrate the existence of two mobility groups: (i) lipids that are transiently trapped by their neighbors and (ii) lipids with displacements on the scale of intermolecular spacing. Most significantly, these mobility groups spatially segregate and form dynamic clusters. The size-scale (1−10 nm) of these clusters is comparable to that of many proteins and other biomolecules; the clustering time-scale (1−2 μs) is similar to that of biological processes such as short enzymatic turnover and protein folding events,[1,38] leading to the possibility that this dynamic heterogeneity plays a functional biological role. The dynamical clusters are very similar to those that occur in glass-forming systems where the clustering is distinct from thermodynamic phase separation.

The length and time scales of these dynamical clusters accord well with those argued to occur in much debated "lipid rafts",[39] which are thought to be essential for the function of living membranes. This commensurability of length and time scales is probably not accidental and suggests that this intrinsic lipid heterogeneity may play a role in the formation of dynamic raftlike structures in cell membranes. Looking forward, the investigation of more complex membrane models should help establish a comprehensive framework to describe lipid dynamic association within membranes and its relation to rafts. We view the present work as an initial step in this direction, and the results provide a reference point for understanding the heterogeneous dynamics of multicomponent membranes.

MODEL AND SIMULATIONS

The MARTINI model for lipids offers a balance of computational efficiency and chemical detail and has been systematically parametrized to reproduce the thermodynamic properties of lipid membranes.[36] The model is based on a four-to-one mapping, where an average of four "heavy" atoms are represented by a single interaction site. For DPPC, the phosphatidylcholine headgroup comprises two charged hydrophilic groups. The glycerol ester component of the lipid is modeled with two sites of intermediate hydrophilicity. Each fatty acid chain, or lipid tail, is modeled by four hydrophobic particles, representing 16 methylene or methyl units. While the MARTINI model is able to capture the sequence of phase transitions observed experimentally,[40] it should be noted that in the gel phase, the MARTINI model does not readily form a tilted phase ($L_{\beta'}$, the prime denoting tilt), so that our gel phase (L_β) is not tilted. Detailed comparisons to experimental observations have been made for lateral diffusion rates,[40] pressure−area isotherms,[41,42] and areal densities.[36] Therefore, the MARTINI model offers an opportunity to quantitatively study the dynamics of lipid systems without the computational costs of more detailed atomistic models.

We use molecular dynamics (MD) simulations to examine the thermodynamics, structure, and dynamics of the MARTINI model for DPPC. All simulations are performed using GROMACS,[43] the standard package used to implement the MARTINI model. Due to the considerable size of dynamical structures, we simulate a rather large system. Specifically, we use N = 2660 DPPC lipids (1330 per membrane layer), hydrated by 85 120 MARTINI water molecules, corresponding to a water/lipid ratio of 32:1, consistent with the experimentally determined ratio.[44] We use periodic boundary conditions to minimize finite-size effects. Simulations are performed with fixed average temperature T and pressure P. In accord with previous MARTINI studies, long-ranged Coulombic forces were truncated at 1.2 nm, and we use an integration time step δt = 0.02 ps.[36] Temperature and pressure were controlled via a Berendsen thermostat and barostat, respectively, both with time constants of 1.0 ps. The simulations were performed at fixed semi-isotropic pressure P = 0. Semi-isotropic pressure coupling allows for the xy plane (the membrane plane) to be scaled independently of the z-axis (membrane normal), which mimics the natural state of bilayers better than uniform, or isotropic, pressure scaling. In this way the surface tension, which is defined by the difference between lateral and transverse pressure, is zero; thus we have tensionless membranes. Under these conditions, the resulting simulation cell has mean dimensions in the membrane plane of ≈25 nm in the ordered gel phase.

We performed preliminary simulations of 1 μs in duration to equilibrate bilayers at six different temperatures between T =

DOI: 10.1021/acs.jpcb.6b02982
J. Phys. Chem. B 2016, 120, 5172−5182

295 K and T = 320 K. Systems were prepared from either a uniform low or high density state, to avoid the potential problem of coexisting phases due to an incomplete phase transition. Since the fluid−gel transition exhibits considerable hysteresis, we can obtain both L_α and L_β systems at T = 305 and 310 K. We discard the data for systems that experience a phase transition. After equilibration, each system was simulated for an additional 1 μs, during which trajectory data were saved for the analysis we present. On the basis of the number of lipids and simulation duration, we can probe size (≈1−10 nm) and time scales (on the order of μs) expected for dynamically associating regions in membranes.

MEMBRANE STRUCTURE AND THERMODYNAMICS

As a preliminary to our study of the membrane dynamics, we briefly characterize of the thermodynamics and structure of our simulated DPPC membranes, which are consistent with prior MARTINI simulations for DPPC.

Simple lipid membranes are characterized by a sequence of phases that depend on temperature, pressure, and hydration.[45,46] On cooling, the main phase transition occurs from fluid phase (L_α) with very little order to a much denser gel (L_β), which is less fluid and exhibits substantial local ordering. (The term "gel" is somewhat misleading, since the system does remain fluid but only on much larger time scales; nonetheless, the term is standard convention.) The common order parameter defining these phases is the lipid areal density, and Figure 1a shows the mean area per lipid A as a function of temperature. The L_α−L_β phase transition occurs between temperatures 305 and 310 K; metastability of the phases results in modest hysteresis of the transition upon cooling or heating of the membrane.[47] As expected, the L_β phase is substantially denser than the L_α phase, and Figure 1b also confirms that tails are more oriented in the L_β phase. Specifically, we quantify the lipid orientation via an orientational order parameter,

$$\langle S \rangle = \frac{1}{2}(\langle 3u_z^2 \rangle - 1) \quad (1)$$

where u_z is the z-component (normal to the membrane plane) of the unit vector of the lipid from the end of its tails to its phosphatidylcholine headgroup. $\langle S \rangle$ = 1 corresponds to alignment perpendicular to the plane of the membrane, while $\langle S \rangle$ = 0 corresponds to an isotropic system. As noted in the modeling section, the gel phase of the MARTINI model is untilted so that $\langle S \rangle$ is nearly 1. If the gel phase were tilted, we would expect $\langle S \rangle \approx 0.62-0.75$, corresponding a tilt of 25−30°.[48]

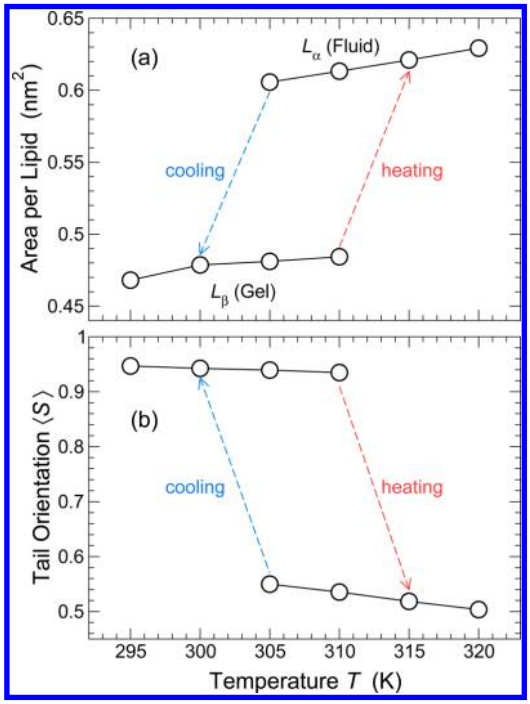

Figure 1. (a) The area per lipid A demonstrates a phase transition from a fluid (L_α) to a gel (L_β) phase between temperature T = 305 K and T = 310 K. Metastability leads to hysteresis of the transition between cooling and heating. (b) The lipid tail orientational order parameter $\langle S \rangle$ shows an increase in tail orientation of lipids along the axis perpendicular to the membrane surface for the L_β phase relative to the L_α phase.

Our later analysis of spatially correlated motions will require structural information, and these data are part of the general characterization of the membrane phases. Accordingly, we evaluate in-plane radial distribution function $g(r)$, also known as the pair-correlation function, for the DPPC center-of-mass separation r (Figure 2a). As expected, the $g(r)$ in the L_α phase shows only weak correlations in DPPC positions, while the L_β phase shows substantial ordering of lipids. Due to the asymmetry of DPPC molecules, nearest neighbor lipids can pack in a variety of orientations; consequently, the first three peaks of $g(r)$ all correspond to nearest neighbor lipid molecules. This splitting of the peak has been experimentally observed in other lipid systems.[49] This will be important later, as we need to identify first neighbors, which we define as those lipids with a center-of-mass separation less than the third minimum of $g(r)$ in the gel phase, which occurs at $r \approx 1.02$ nm.

The Fourier transform of $g(r)$ yields the static structure factor $S(q)$ as a function of wave-vector magnitude q. $S(q)$ is directly measured experimentally and is sensitive to periodicity of structure. Figure 2b demonstrates that these membranes are indeed amorphous, due to the lack of Bragg peaks. However, a significant increase in the ordering of the L_β gel phase is apparent from the features located at q_0 = 14, $\sqrt{3}q_0$, and $2q_0$. These features are commonly observed in what is known as a 2D hexatic phase, an intermediate between crystal and isotropic liquid phases, and includes the presence of defects that disrupt long-range translational order. The hexatic phase is well-characterized in 2D fluids,[50] and previous studies of lipid bilayers also indicate that the high-density phase shares many similarities to this phase.[18,40,42,51]

MEMBRANE DYNAMICS

As a prelude to considering correlations in lipid displacements, we first characterize the average single-molecule dynamical properties. To quantify mean lipid mobility, we evaluate the in-plane mean-squared displacement $\langle r^2(t) \rangle$ of the center-of-mass of lipid molecules (Figure 3a). It is immediately apparent that $\langle r^2(t) \rangle$ separates into two distinct groups, which correspond to the L_α and L_β phases. For both phases, $\langle r^2(t) \rangle \sim t^2$ for very short intervals ($\lesssim$1 ps), corresponding to ballistic motion, expected on scales less than the mean collision time.

For the fluid L_α phase, $\langle r^2(t) \rangle$ transitions to linear time dependence, or normal diffusion behavior, at large time intervals; at an intermediate time scale that spans about 2 decades, there is a subdiffusive regime in which displacement

DOI: 10.1021/acs.jpcb.6b02982
J. Phys. Chem. B 2016, 120, 5172−5182

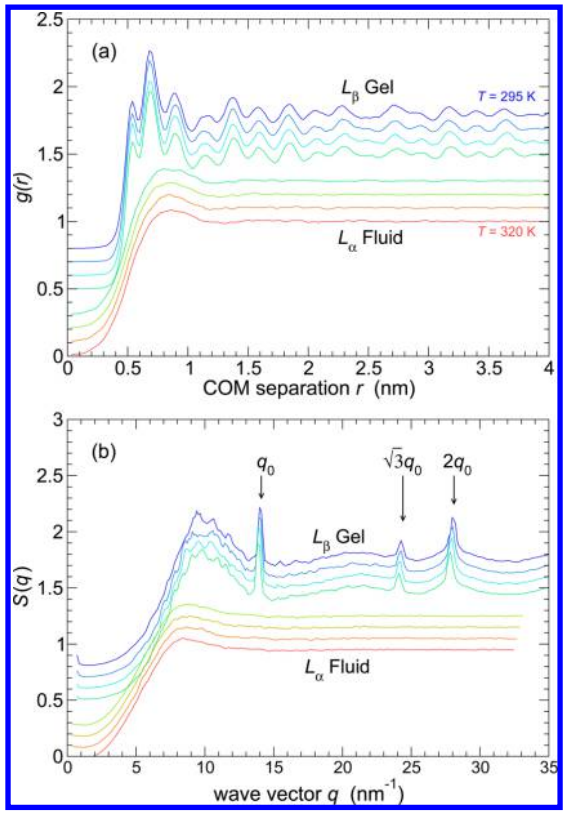

Figure 2. (a) In-plane radial distribution function of lipids within the membrane in the L_α and L_β phases. The oscillations in the gel and L_β phase indicate long-ranged order, which are notably absent in the L_α phase. Curves are shifted vertically for clarity in this figure; lowest T is at the top, highest T is at the bottom; temperatures follow Figure 1, where we remind the reader that we can observe both L_α and L_β phases at T = 305 and 310 K. (b) In-plane structure of the membrane lipids quantified through the static structure factor in the L_α and the L_β phases. The L_β phase displays hexatic ordering of the lipids, as indicated by the presence of sharp features in $S(q)$ indicated by the arrows. Curves are shifted vertically for clarity; lowest T is at the top, highest T is at the bottom.

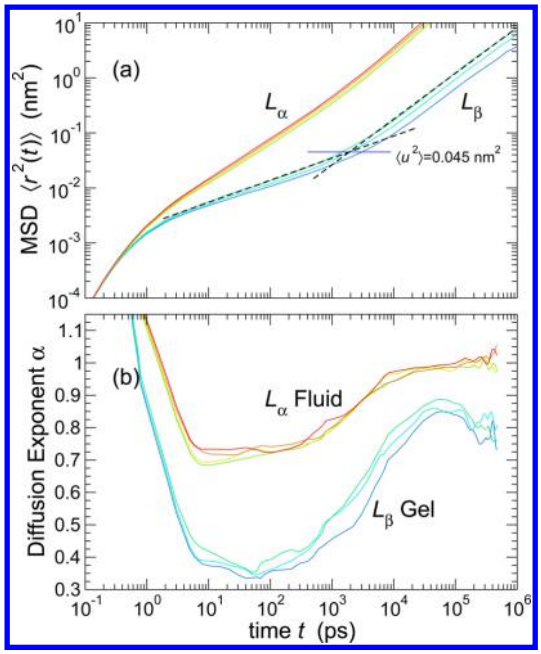

Figure 3. (a) In-plane mean-squared displacement $\langle r^2(t)\rangle$ for lipids. There is a notable gap in $\langle r^2(t)\rangle$ crossing the L_α–L_β phase transition. In the L_β gel phase, $\langle r^2(t)\rangle$ exhibits a "plateau"-like region over a substantial t-range, indicative of transient "caging". This plateau is ubiquitous in fluids approaching a glass transition. The heavy dashed lines show subdiffusive behavior $\langle r^2(t)\rangle \sim t^{0.35}$ at intermediate t that crosses over to a nearly diffusive behavior $\langle r^2(t)\rangle \sim t^{0.85}$ at larger t. The intersection of the dotted lines defines a characteristic scale $\langle u^2\rangle$ = 0.045 nm^2. (b) Instantaneous value of the anomalous diffusion exponent α, defined by eq 2. Even in the L_α fluid phase, there is an anomalous region from ∼10 to 500 ps where $\alpha \approx 0.7$. In the gel L_β, the more pronounced molecular caging yields a smaller $\alpha \approx 0.35$. Even approaching 1 μs, the L_β phase does reach the diffusive limit, and instead $\alpha \approx 0.85$.

grows sublinearly. In the transient subdiffusive regime, the displacement follows a power law $\langle r^2(t)\rangle \sim t^\alpha$, where α is sometimes referred to as the anomalous diffusion exponent. The instantaneous value for α can be defined from the logarithmic slope of displacement,

$$\alpha(t) \equiv \frac{\mathrm{d}\ln\langle r^2(t)\rangle}{\mathrm{d}\ln t} \tag{2}$$

Figure 3b shows that in this intermediate regime, $\alpha \approx 0.7$ until about 100 ps, whereupon displacement returns to normal diffusion with α = 1; these values are very similar to those reported for the fluid phase of DSCP, SOCP, and DOCP in all-atom studies.[52] This type of "anomalous" transport is well documented,[52−56] but the present work emphasizes correlated dynamics that cannot be captured using only a consideration of single lipid molecule displacements.

The lipid mobility in the gel L_β phase is substantially reduced compared to the L_α phase, and the displacement exhibits a more pronounced subdiffusive regime, where $\alpha \approx 0.35$. At larger time, the exponent α does not recover diffusive behavior and asymptotes to $\alpha \approx 0.85$ over the 1 μs scale. At even larger time scales than accessed here, the lipid displacement process should return to ordinary diffusion. This pronounced subdiffusive regime is qualitatively similar to simulations of DSPC in the gel phase.[52] Such strong subdiffusive behavior is also a canonical feature of glass-forming fluids[3,4,30,31] and other amorphous materials when thermal energy becomes small relative to the molecular interactions. This phenomenology can be naturally expected to occur in the dense lipid phases where the molecules are strongly interacting while at the same time exhibiting a degree of disorder, so that intermolecular interactions are strongly anharmonic. In this subdiffusive regime, the crowding of nearest-neighbors leads to transient "caging" of lipid molecules that hinders the diffusion process. As noted before, lipids eventually escape from the cages that arise from interactions with their neighbors, and the system gradually crosses over to diffusive behavior. Clearly, this is a cooperative phenomenon that goes beyond simple diffusion, and understanding the distinction between lipids that are transiently trapped and those that have found pathways for motion will provide a quantitative picture of dynamical heterogeneity in the membrane.

To link more directly to experimental measurements of lipid mobility, we extract the in-plane diffusion coefficient from the Einstein relation in 2D,

$$D = \lim_{t\to\infty} \frac{\langle r^2(t)\rangle}{4t} \tag{3}$$

DOI: 10.1021/acs.jpcb.6b02982
J. Phys. Chem. B 2016, 120, 5172−5182

in the regime where $\langle r^2(t)\rangle$ grows linearly. Since $\langle r^2(t)\rangle$ never fully recovers linear behavior in the gel phase within the time scale of our simulations, our estimates for D of the gel are an upper bound,[57] but this does not detract from the qualitative implications of the findings. Figure 4 shows a discontinuous

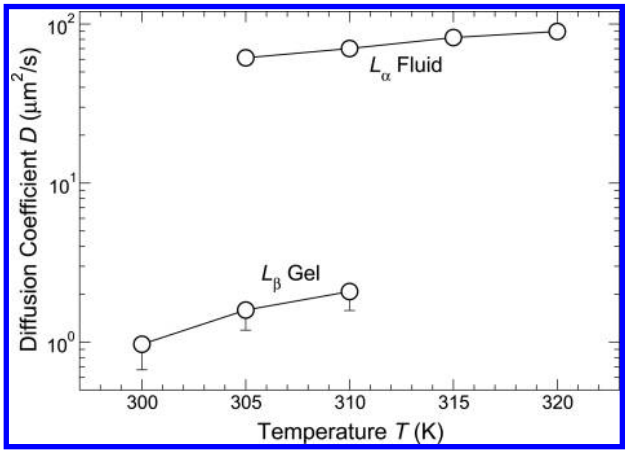

Figure 4. Lateral diffusion coefficient D extracted from the asymptotic behavior of $\langle r^2(t)\rangle/(4t)$. The transition to the L_β phase is marked by a dramatic drop in the value of D, and the D values for the gel phase should be considered upper bounds.

drop in D crossing the L_α–L_β transition by a factor of 10, consistent with experimental results.[58] The time scales of the MARTINI model are known to be 2- to 10-fold faster than experiments.[40] This speeding up of the dynamics is a consequence of coarse-graining the molecular description of the molecules. A comparison between Figure 4 and experiments[58] indicates that D values in our simulations are ≈6 times greater than those determined through experiments. Therefore, we anticipate that experimental time scales should be roughly 6 times larger, and we revisit this issue in the Conclusions section.

Given the similarities between the behavior of $\langle r^2(t)\rangle$ in the gel phase with that observed for glass-forming fluids, we are motivated to examine if the theoretical framework and tools traditionally used in glass formation are useful to understand the variations in membrane mobility. Thus, as a first step, we examine the degree to which the molecular displacements that determine $\langle r^2(t)\rangle$ conform to a Gaussian distribution. For ballistic or diffusive regimes, the displacements must follow a Gaussian function. During the transient caging regime in glass-forming systems, the displacements typically do not follow a Gaussian distribution. In these strongly interacting fluids, the degree of deviation is commonly quantified through the non-Gaussian parameter $\alpha_2(t)$, defined in 2D as

$$\alpha_2(t) = \frac{\langle r^4(t)\rangle}{2\langle r^2(t)\rangle^2} - 1 \tag{4}$$

For systems with a Gaussian distribution of displacements, $\alpha_2(t) = 0$. (The non-Gaussian parameter α_2 should not be confused with α, the anomalous diffusion exponent, although both provide an indication of non-Brownian dynamics.) Figure 5 shows that for the L_α phase $\alpha_2(t) \approx 0$ for all t, consistent with lipid molecular motions that conform to Brownian statistics; this is true even in the regime where the anomalous diffusion exponent $\alpha \approx 0.7$. This finding is consistent with the all-atom studies of ref 52, where where they considered the ratio $\langle r^4(t)\rangle/\langle r^2(t)\rangle^2$. In contrast, in the L_β gel phase $\alpha_2(t)$ exhibits a pronounced peak, indicating that displacements are highly non-Gaussian during the time that $\langle r^2(t)\rangle$ shows transient caging and begins to return to diffusive behavior. The peak of $\alpha_2(t)$ occurs at roughly the same characteristic time t^* for all T in the L_β phase. At large t, $\alpha_2(t)$ decreases toward zero, consistent with approaching linear (diffusive) growth of $\langle r^2(t)\rangle$.

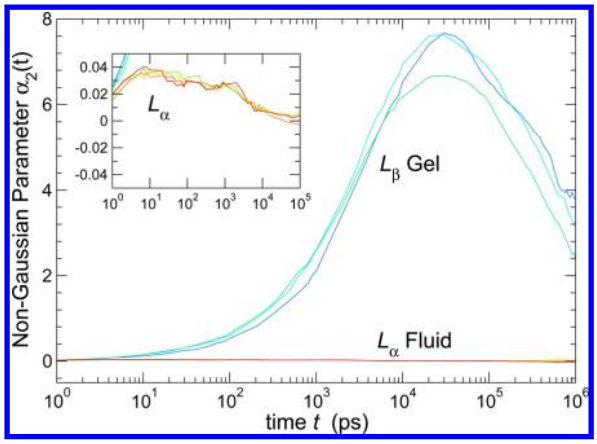

Figure 5. Non-Gaussian parameter $\alpha_2(t)$ for the L_α and L_β phase. While α_2 is near zero for the L_α phase, significant growth can be seen in the L_β phase in the same t-range that $\langle r^2(t)\rangle$ shows a subdiffusive behavior. $\alpha_2(t)$ has a characteristic time t^* when displacements show the largest deviation from a simple Gaussian distribution, which does not vary significantly with T in the L_β phase. The inset expands $\alpha_2(t)$ for the fluid L_α phase, demonstrating that it is nearly zero for all t.

MEMBRANE DYNAMICAL HETEROGENEITY

The presence of non-Gaussian displacements indicates an alternative mechanism for molecular displacements but does not provide an explanation of its physical origin. One proposal is that molecular displacements are homogeneous and described by a fractional Langevin equation.[52] On the other hand, in both glass-forming fluids and the hexatic phase of 2D fluids, non-Gaussian behavior occurs due to inhomogeneous spatial correlations in the motions of a fraction of molecules in the system. This mobile fraction exhibits enhanced mobility from the rest of the system, and these molecules typically cluster together spatially − the phenomenon of dynamical heterogeneity. We now consider this possible scenario.

Distinct Mobility Groups. In order to quantify the nature of non-Gaussian displacements and develop a model description, we explicitly examine the distribution of center-of-mass displacements r at a given time t, better known as the self-part of the van Hove correlation function $G_s(r,t)$.[59] We evaluate $G_s(r,t)$ for the L_β gel phase at the time t^*, since this is when non-Gaussian effects are strongest.

Figure 6 shows $G_s(r,t^*)$ of the gel phase, which has a large peak at small displacements, indicating that the majority of lipids have hindered motion and are only able to sample their local surroundings; $G_s(r,t^*)$ also shows a long "tail", much longer than would be expected from Gaussian displacements of the same mean. This tail extends to displacements beyond nearest neighbor distances, indicating that on the time scale of t^*, a small fraction of lipids are able to escape the cages formed by their neighbors. This should not be confused with so-call "hop-diffusion".

DOI: 10.1021/acs.jpcb.6b02982
J. Phys. Chem. B 2016, 120, 5172−5182

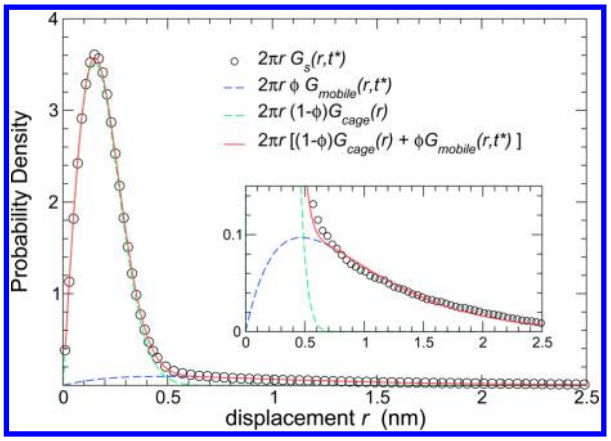

Figure 6. van Hove function $G_s(r,t^*)$ at the time t^* of the maximum of non-Gaussian behavior for T = 300 K, representative of the gel phase. The van Hove function is well described by the superposition of a Gaussian function, representing low-mobility caged lipids (green line), and an exponential function to represent highly mobile lipids (blue line). The red line indicates that the summation of these terms follows the simulation results (circles) closely. The inset shows the tail of the distribution in enlarged form.

More significantly, we now show that it is possible to quantitatively describe $G_s(r,t^*)$ as a superposition of two distinct mobility groups,

$$G_s(r,t^*) = \phi G_{\mathrm{mobile}}(r,t^*) + (1-\phi)G_{\mathrm{cage}}(r) \quad (5)$$

where ϕ represents the fraction of mobile lipids. We first consider an appropriate form for $G_{\mathrm{cage}}(r)$. We can use $\langle r^2(t)\rangle$ to define a characteristic displacement scale $\langle u^2\rangle$ of the transiently trapped lipids. Specifically, the crossover over from subdiffusive behavior with α = 0.35 to α = 0.85, indicated by the intersection of the dashed lines in Figure 3a, defines $\langle u^2\rangle$ = 0.045 nm^2 and does not depend significantly on T. Assuming Brownian motion of the caged lipids with mean $\langle u^2\rangle$, the van Hove of these particles should obey a Gaussian function,

$$2\pi r G_{\mathrm{cage}}(r) = \frac{2r}{\langle u^2\rangle} e^{-r^2/\langle u^2\rangle} \quad (6)$$

Figure 6 demonstrates $(1-\phi)G_{\mathrm{cage}}(r)$ describes the primary peak of $G_s(r,t^*)$, where ϕ is the only adjustable parameter.

The tail of $G_s(r,t^*)$ is associated with those lipids that are highly mobile and are able to escape their local surroundings. In glass-forming fluids, the tail of $G_s(r,t^*)$ is often described as an exponential function,[60]

$$2\pi r G_{\mathrm{mobile}}(r) = \frac{r}{r_0^2} e^{-r/r_0} \quad (7)$$

Indeed, we find that the tail of $G_s(r,t^*)$ exhibits the signature exponential tail of many glass-forming liquids. Fitting the tail of $G_s(r,t^*)$ determines values for r_0 and ϕ; the value of ϕ estimated for mobile particles is consistent with the fraction $(1-\phi)$ of caged lipids in the superposition expression for $G_s(r,t^*)$ (eq 5). In sum, the only free parameters in the superposition description are the values of ϕ and r_0, since $\langle u^2\rangle$ is determined from $\langle r^2(t)\rangle$. The fraction ϕ of these mobile particles varies around a mean value of 14.2% with standard deviation of 2.7%. We find r_0 values between 0.55 and 0.71 nm so that the mean mobile lipid $\langle r_{\mathrm{mobile}}{}^2(t^*)\rangle^{1/2} = 2r_0$ varies from 1.1 to 1.4 nm, slightly larger than the intermolecular spacing (1.02 nm). In other words, a typical mobile lipid moves on the order of a molecular spacing on this time scale, suggesting that a molecular "replacement" mechanism may be at work.

In short, we have so far shown that the DPPC molecular displacements are starkly different in the fluid L_α and gel L_β phases; in particular, lipid displacements are non-Gaussian in the gel phase, due to the existence of two mobility subpopulations: lipids that are trapped in cages formed by their neighbors and a fraction ϕ of lipids that escape their cages and move beyond the space between neighboring lipids. We next examine the structure of these relative mobility groups. We will emphasize how this dynamic, interchanging population of mobility subsets can naturally arise without invoking concepts of thermodynamic phase coexistence, just as they commonly occur in glass-forming materials.

Cluster Size. Having established that single lipid motion in the gel phase can be partitioned into two groups at the intermediate time scale of subdiffusive motion, we now examine the spatial distribution of this heterogeneity. To provide a useful qualitative picture of the consequences of this heterogeneity, Figure 7 shows a simulation snapshot of the

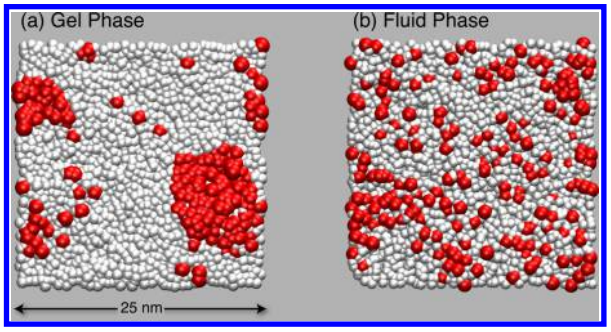

Figure 7. Representative snapshots of one side of the bilayers at (a) T = 300 K and (b) T = 320 K. Mobile lipids are colored red, while caged lipids are white. We use only the centers of mass of the lipids to facilitate visualization; mobile lipids are drawn slightly larger than immobile ones. In the fluid L_α phase there are no distinct mobility classes, and the fraction of the most mobile lipids are randomly dispersed. In the gel L_β phase there are strong spatial correlations between the fraction ϕ of mobile lipids.

lipid centers-of-mass, looking down at one layer of the membrane; beads are colored according to whether lipids are mobile (red) or caged (white) over the time interval t^*. This figure clearly shows that the mobile fraction (ϕ) of the lipids is highly spatially correlated in the gel phase, leading to substantial clustering of mobile lipids within a background of caged lipids. Although this image is highly remiscent of phase coexistence of the L_α and L_β phases, we shall provide evidence that these clusters are not associated with phase segregation. We observe that such clusters can span at least 10 nm, putting them on a size scale comparable with proteins and many cell membrane constituents. By way of comparison, we highlight the same fraction of the most mobile lipids in the L_α phase and show that these mobile lipids are essentially randomly distributed in the membrane. This is consistent with the Brownian nature of displacements in the fluid L_α phase, which assumes that single particle displacements occur independently. Accordingly, spatial correlations of mobility appear only in the gel phase.

We now proceed to quantify the size of clusters formed by mobile lipids in the gel phase. We define a cluster as those mobile lipids that are nearest neighbors, where nearest

DOI: 10.1021/acs.jpcb.6b02982
J. Phys. Chem. B 2016, 120, 5172−5182

neighbors are defined as those having a separation less than 1.02 nm, a criterion discussed when we examined the pair-correlation function $g(r)$ (see Figure, 2a). Up to now, we have defined these clusters only for displacements on the time interval t^*. We can trivially generalize this approach by looking at the same fraction ϕ of the most mobile lipids at any arbitrary time interval t and thus evaluate the mean cluster size $\langle n(t)\rangle$. For very short intervals (where lipid motion is ballistic) or after long intervals (where motion is nearly diffusive), single lipid motions are independent. Thus, partitioning mobility groups should reveal spatial correlations of mobility only on an intermediate time scale. Figure 8a confirms this expectation. At very short times, $\langle n(t)\rangle \approx 2$, trivial clusters that arise due to a random choice of a fraction of lipid molecules. The maximum cluster size at these thermodynamic conditions occurs on a time interval that is slightly larger than t^* so that the clustering is most pronounced at a time scale in the range t = 150−300 ns. On the basis of the correspondence between the diffusion constants in the simulation and experiments, we expect this to map to an experimental time scale in the range $t \approx 1-2$ μs.

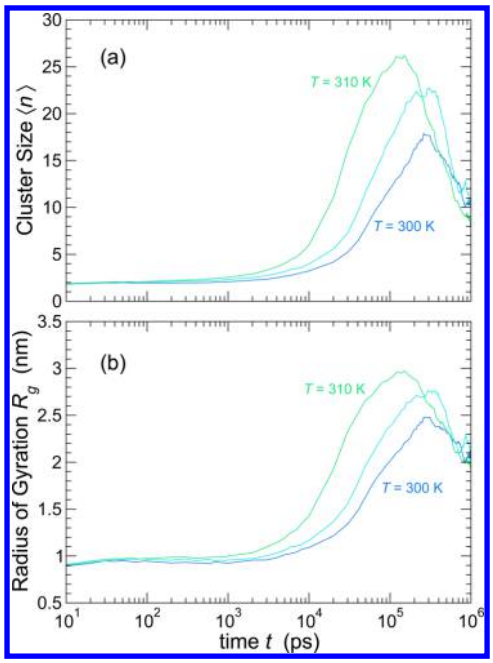

Figure 8. (a) Mean cluster size $\langle n(t)\rangle$ of the fraction ϕ of the mobile lipids as a function of t. Clustering is most pronounced on the time scale near that of the peak time $t^*$of $\alpha_2(t)$. As the system reaches the long-time diffusive regime, the clustering diminishes as Brownian motion begins to dominate. (b) Radius of gyration R_g as a function of time t. It is most pronounced when $\langle n(t)\rangle$ reaches its peak and diminishes when system begins to approaches diffusive behavior.

A characteristic maximum value of $\langle n(t)\rangle$ similarly occurs in a simpler lipid membrane model[18] and this feature is general in glass-forming liquids. A curious feature of Figure 8 is that the maximum cluster size monotonically decreases on cooling, while the value normally increases on cooling for the case of glass-forming systems. On the other hand, an enhancement of clustering upon heating has been documented for the atomic motions of crystals approaching their melting transition;[61] these crystals also exhibit the same type of two-state description of mobility groups. As in the case of crystal melting, the proximity to the L_α−L_β phase transformation may serve to enhance the size of heterogeneous regions, an effect that also likely enhances molecular transport of any embedded molecules near the transition. Jin et al.[62] have observed a strong enhancement of diffusion in the membranes of lipids extracted from *E. coli* driven by growth temperature, and they have suggested that this phenomenon arises from some sort of fluctuations in the membrane.

To characterize the length scale of these dynamic clusters, we evaluate the mean radius of gyration, which for a given cluster is defined by

$$R_g^2(t) = \frac{1}{2N^2}\sum_{i,j}(r_i - r_j)^2 \tag{8}$$

where r_i, r_j are the positions of the center-of-mass of lipids within a cluster defined over interval t. As should be anticipated, Figure 8b shows that $\langle R_g(t)\rangle$ of mobile lipid clusters exhibits the same trend observed for $\langle n(t)\rangle$. In particular, $\langle R_g\rangle$ has a peak value around 2.5−3 nm so that the average size of a mobile clusters is comparable to many proteins and other biomolecules. Obviously, specific clusters can be larger or smaller, as illustrated in Figure 7. For the simpler lipid model that we examined in ref 18, we found that the cluster size distribution followed a power law with an exponential cutoff, a behavior consistent with percolation theory.[63] A broad size distribution is a rather generic finding in the assembly of branched particle aggregates. The peak $\langle R_g(t)\rangle \approx 3$ nm is consistent with a peak $\langle n(t)\rangle \approx 30$, if we approximate clusters as compact 2D objects and use the interlipid spacing of ≈1 nm. In fact, these objects are probably not compact, and ref 18 suggests they have a slightly smaller fractal dimension $d_f \approx 1.9$, the fractal dimension of critical percolation clusters in 2D.[63] We lack sufficient data to accurately estimate d_f here, so this remains an open question.

Cluster Structure. A natural question that arises from this analysis is the following: How do the structures of these mobility groups compare, and are they related to the structure of the fluid L_α and gel L_β phases? For example, one might anticipate that these patches arise from a thermodynamic coexistence of a fluid patches within the gel phase, and so we examine the degree to which we can identify structural differences in the mobile and immobile domains. Since the area and tail orientation of lipids differ substantially between the gel and fluid phases, these may be good metrics to assess the variation in structure of mobile and immobile regions.

We quantify the area occupied by a lipid using the area of the Voronoi cell, where the Voronoi mesh is constructed from the 2D projection of the center of mass locations of lipids in each layer of the membrane. A Voronoi cell specifies the region closer to a given lipid than to any other lipid in the layer. Figure 9 (a, b) shows typical examples of the Voronoi mesh for both the gel and fluid phases. In the fluid phase, the spatial distribution of the cell areas does not exhibit an obvious pattern. In contrast, in the gel phase, regions of relatively larger area are spatially correlated. A comparison to the mobile regions shown in Figure 7 (based on the same configuration) shows that these lower density regions of the material correlate well with the locations of regions of enhanced mobility. This suggests the possibility of using the local structure to identify regions of differing mobility, a possibility that we test below. To quantify the differences in the local density of mobile and caged regions and thus address the possibility of phase coexistence, we explicitly evaluate the distribution of areas $P(A)$ for lipids that were identified as mobile or caged, as well as for the overall

DOI: 10.1021/acs.jpcb.6b02982
J. Phys. Chem. B 2016, 120, 5172−5182

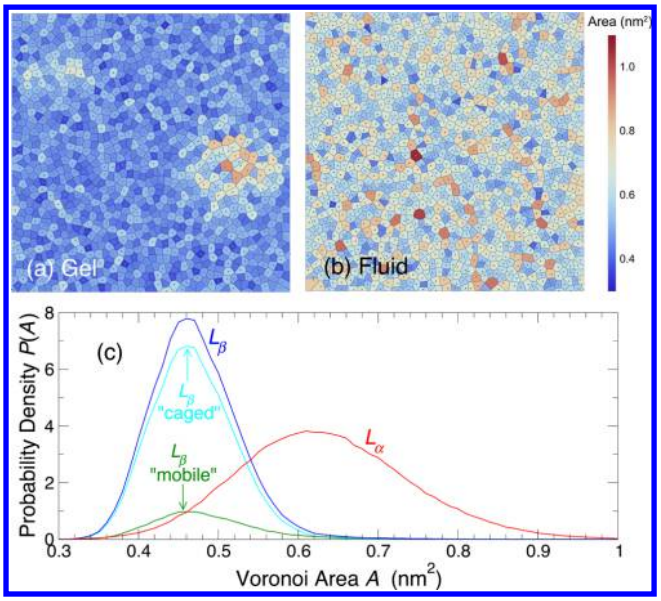

Figure 9. Typical examples of the Voronoi mesh for (a) the gel phase and (b) the fluid phase. Cell coloring denotes area (see scale to the right), and the dots indicate the locations of the centers of mass for each lipid. Spatial correlations of area are more pronounced in the gel phase. (c) Distribution $P(A)$ of Voronoi area A for the fluid and gel phases. In addition, we separate the contributions to $P(A)$ of mobile and immobile lipids in the gel phase. $P(A)$ for mobile lipids in the gel phase is clearly distinct from that of the fluid phase.

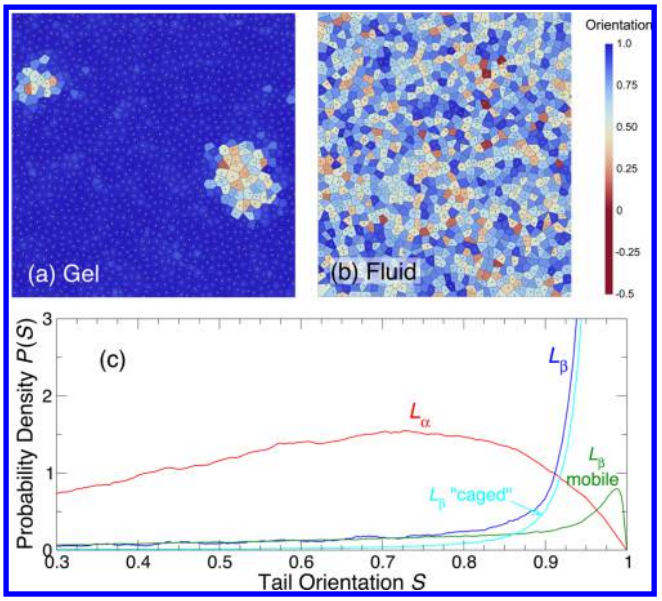

Figure 10. Typical examples of the spatial variation of lipid tail orientations for (a) the gel phase and (b) the fluid phase. We use again use the Voronoi mesh, but here cell coloring denotes orientation (see scale to the right), and the dots indicate the locations of the centers of mass for each lipid. Spatial correlations of area are visibly distinct in the gel phase. (c) Distribution $P(S)$ of tail orientations S for the fluid and gel phases. In addition, we separate the contributions to $P(S)$ of mobile and immobile lipids in the gel phase. There is overlap of the $P(S)$ distributions for mobile and immobile lipids in the gel phase, but nearly all lipids with $S < 0.9$ are mobile.

fluid and gel phases. Figure 9c shows that while mobile lipids are skewed to somewhat larger areas, the mean area for mobile lipids is only about 5% larger than that of the gel phase. Moreover, the distribution of mobile lipid areas is notably different from that of the fluid phase, so these mobile regions do not correspond to phase coexistence with the fluid phase.

We carry out a similar analysis to the above for the tail orientation, which we define by the lipid tail orientational order parameter S, given in eq 1 (without averaging over lipids). Figure 10 (a, b) shows typical examples of the lipid orientation for both the gel and fluid phases, partitioned using the same Voronoi mesh for comparison. Like the Voronoi areas, regions of relatively low orientation are spatially correlated in the gel phase, and the effect appears much more pronounced than for the lipid area. In the gel phase, caged lipids have a value of $\langle S \rangle = 0.96$, while the mobile lipids in the gel phase have $\langle S \rangle = 0.71$, a substantially larger difference than observed for area (≈25% versus ≈5%). Similar to the case of area, mobile lipids in the gel phase are still far more oriented than those of the fluid phase (where $\langle S \rangle \approx 0.50-0.55$). We more carefully dissect these differences by evaluating probability distribution $P(S)$ of tail orientation values. Figure 10c shows that S values for the gel phase are very narrowly distributed near $S = 1$, while for the fluid phase, S values are extremely broad, with a weak peak around $S = 0.75$. The mobile regions have a considerably broader distribution of S values than the caged regions, but both still peak near $S = 1$. Moreover, $P(S)$ for the mobile regions of the gel phase is distinct from that of the fluid phase, further supporting that these are not regions of thermodynamic phase separation. The different mobility clusters do not appear to represent coexisting phases but instead reflect local differences in ordering within a single thermodynamic phase.

Even if these clusters are not associated with phase separation, the variations in the local area, and especially the tail orientation, of mobile and caged lipid molecules suggest that these local structural measures might be sufficient to distinguish these mobility groups. To test this possibility, Figure 11 compares the spatial distribution of the fraction $\phi = 0.142$ of (a) the most mobile lipid molecules over the interval t^*, (b) the lipids with the smallest tail orientation S, or (c) the largest Voronoi cell area A. All extremes give rise to a degree of clustering, but it is visually apparent that the degree of clustering is strongest based on mobility and is weakest based on local area; the clusters of highly mobile lipids show a strong similarity to those having the least tail orientation. The normalized covariance of the mobility (measured by displacement) with tail orientation S is quite large, 0.943, while the covariance of mobility with area A is considerably weaker, 0.346. Thus, tail orientation provides a helpful indicator of the underlying dynamical heterogeneity, while local area is only modestly useful as a structural indicator of dynamics. Murtola et al.[12] found evidence for a similar relationship between local mobility with density or orientation. This relationship between orientation and mobility is practically beneficial, since the detailed procedure to identify mobility groups is not currently accessible to experiments, although single molecule tracking methods offer a promising future approach. On the basis of the strongly hexagonal order in the gel phase,[18,42] other measures of local order, such as the hexagonal rotationally invariant order parameter Q_6,[64] could also be sensitive to changes in local mobility.

CONCLUSIONS

We used the MARTINI model to examine the heterogeneity of dynamics in a simulated DPPC lipid membrane. Our results support the findings of a previous work based on a more

DOI: 10.1021/acs.jpcb.6b02982
J. Phys. Chem. B 2016, 120, 5172−5182

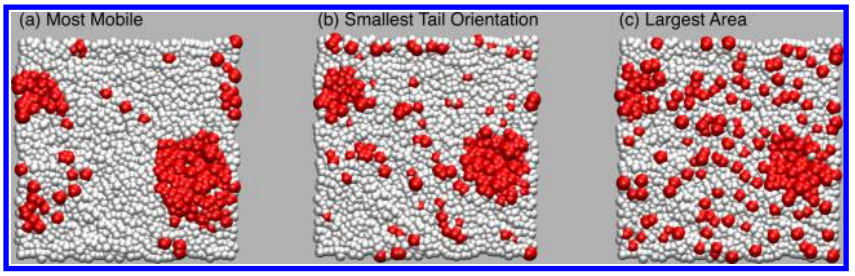

Figure 11. Visualization of the clusters formed in the gel phase by highlighting the same fraction ϕ of (a) the most mobile lipid molecules, (b) the lipids with the smallest tail orientation S, and (c) lipids with largest Voronoi area A. The configuration used is the same as Figure 7. In each case, the highlighted fraction ϕ is shown in red, with the counterpart in white. It is apparent that the mobility groups can, in large part, be distinguished on the basis of their local tail ordering and to a lesser extent by local density.

coarse-grained lipid model with nonspecific lipid interactions.[18] We showed that in the gel phase, subdiffusion arises due to transient caging of lipid molecules by neighboring molecules, resulting in non-Brownian motion of the lipid molecules. This phenomenon is accompanied by the coexistence of two distinct mobility subpopulations: low-mobility lipids that have slight enhancement in orientational order and are trapped in cages formed by their neighbors, and a smaller fraction of mobile lipid molecules that have a comparatively low local orientational order.

Of particular significance for membrane dynamics, the particles in these extreme mobility groups have strong spatial correlations, in the form of self-assembled dynamic clusters that do not appear to be associated with the phase separation process. While a significant correlation exists between tail orientation and lipid mobility, the mobile lipid clusters are not consistent with patches of lipids existing in the fluid L_α phase. Instead, these clusters appear to be a manifestation of dynamic heterogeneity, a phenomenon observed in many condensed-matter systems, particularly glass-forming fluids. In terms of time and size scale, these clusters are most prominent at 1−2 μs (accounting for the shift to experimental time scale) and have a characteristic size of 1−5 nm, but specific clusters can be as large as 10 nm.

Given the inherent sluggishness of dynamics in the gel phase, a natural concern is whether our results are affected by insufficient equilibration in the gel phase. Indeed, a poorly chosen initial state can affect quantitative findings on the μs time scale we simulate. That said, the ubiquity of the dynamic heterogeneity in condensed phase systems indicates it is a rather robust phenomenon when intermolecular interactions are strong compared to thermal excitation.[3,4,30] Hence, the qualitative features of heterogeneity are likely not strongly sensitive to the details of equilibration. Additionally, the qualitative similarity of the dynamics we observe to those found in all-atom studies[52] suggests that our core findings should not be dependent on the details of the lipid representation. Indeed, the general pattern of dynamic clustering is consistently observed in glass-forming systems, independent of the details of the model or system size, and we anticipate a similar scenario for membranes.

The strong correlation between the tail orientation and mobility of individual lipid molecules in the gel phase is somewhat unanticipated. Past studies of glass-forming fluids typically do not indicate any clear-cut correlation between structure and dynamics at the scale of individual molecules.[65] This is a consequence of the fact that distributions of various measures of local order for mobile and immobile molecules overlap substantially, making it difficult to distinguish mobility species solely using measures of local order. In contrast to most glass-forming systems, the proximity to a liquid−liquid phase transition allows the membrane to access dynamic local structures with substantially different ordering, as well as mobility, based on the differences in mean order and diffusivity of the fluid and gel phases. Consequently the distributions of local order (here defined by the tail orientation) of the differing mobility groups are more separated. Presumably, this could also be quantified through strong hexatic ordering of the gel state (Figure 2b). Liquid water, where there is also a possible liquid−liquid transition, is another example where pronounced ordering does give rise to strong correlations between local structure and mobility.[66,67]

The characterization of collective coordinated motion is a separate matter from identifying particles in extreme mobility states. In glass-forming fluids[31] and our earlier membrane study,[18] it has been shown that the clusters of enhanced mobility can be dissected into subgroups of particles that cooperatively replace each other, revealing stringlike collective motions. Indeed, we found that the characteristic displacement of highly mobile lipid molecules corresponds to roughly an interlipid separation, suggesting just such a cooperative exchange motion. Pictorial evidence from Falck et al.[13] also suggests such a scenario. We are then led to the following question: What are the biological implications of this type of collective motion?

Though our specific results are limited to the comparatively simple case of the DPPC membrane, it is valuable to consider the potential broader biological relevance of our findings. As alluded to in the Introduction, the size and time scales of the mobile lipid clusters are consistent with those expected of dynamically associating lipid rafts.[1] However, it is important to note that the situation of highly mobile groups in an immobile environment is inverted from the situation expected for lipid rafts: lipid rafts are usually conceived of as patches of relatively low mobility in a fluid background. Thus, the coincidence in scales may be just fortuitous. On the other hand, the emergence of fluid regions in an ordered background is characteristic of superheated crystals,[61] so this situation certainly has precedence. The dissonance between our observations and expectations for rafts may also be a consequence of examining a single-component membrane. In many glass-forming systems, the appearance of high-mobility clusters is also accompanied by the appearance of low-mobility clusters, usually with similar size and time scales, especially when ordering is frustrated.[31] This type of frustration in ordering is realized, for example, in a simple binary mixture of atomic species having different sizes with interparticle interactions that favor a homogeneous liquid.[68] Real membranes are multicomponent fluids that

DOI: 10.1021/acs.jpcb.6b02982
J. Phys. Chem. B 2016, 120, 5172−5182

must exhibit this type of packing frustration, so these materials may exhibit dynamics more similar to glass-forming liquids. Although the application of results for the single-component membrane to describe cell membranes is necessarily limited, the simple model membrane system is exceedingly valuable as a reference point to build comprehension of more complex living membranes. As a continuation of our "bottom-up" strategy, we are currently working to quantify heterogeneity in multi-component membranes and determine to what degree the compositional heterogeneity affects the intrinsic dynamic heterogeneity of lipid molecules.

We believe that dynamic cluster formation in a single-component lipids membrane is potentially significant for understanding biological function, even if these clusters do not directly relate to lipid rafts. The mobile lipid clusters near the fluid−gel transition are on the order of a few nm and can thus accommodate a number of proteins and other biomolecules within a cluster and persist for a microsecond, comparable to enzyme turnover time and many other biological processes associated with membrane function.[1] The rather general tendency of many types of cells to adjust their composition to bring the membrane near the gel transition seems to point some survival advantage of this critical condition and biological functionality of these dynamic clusters.

We hope that our observation of this general clustering phenomena brings us one step closer toward elucidating dynamical aspects of lipid membranes that have long remained elusive and that our observations will stimulate measurements of this dynamical heterogeneity using NMR and other methods having sufficient time and spatial resolution. Further, the finding of dynamical heterogeneity in lipid membranes points to a general tendency for molecules having strong intermolecular interactions to form large-scale, self-assembled dynamic structures at equilibrium. This opens up the possibility that tools from the field of glass-forming fluids can be further applied to deepen our understanding of lipid dynamics and potentially the dynamics of other complex biological systems, such as proteins. Such a framework may even prove useful to quantify the inherently complex dynamics of biological macromolecules and living systems at even larger scales, such as the dynamics within cells growing tissue.[69,70]

AUTHOR INFORMATION

Corresponding Author

*E-mail: fstarr@wesleyan.edu. Phone: +1 860-685-2044.

Notes

The authors declare no competing financial interest.

ACKNOWLEDGMENTS

We thank C. Othon, R. Nossal, and D. Simmons for discussions. Computer time was provided by Wesleyan University. This work was supported in part by NIST Award 70NANB13H202 and ACS-PRF Grant 51983-ND7.

REFERENCES

(1) Jacobson, K.; Mouritsen, O. G.; Anderson, R. G. W. Lipid rafts: at a crossroad between cell biology and physics. *Nat. Cell Biol.* **2007**, *9*, 7−14.

(2) Simons, K.; Ikonen, E. Functional rafts in cell membranes. *Nature* **1997**, *387*, 569−572.

(3) Ediger, M. D. Spatially heterogeneous dynamics in supercooled liquids. *Annu. Rev. Phys. Chem.* **2000**, *51*, 99−128.

(4) Richert, R. Heterogeneous dynamics in liquids: fluctuations in space and time. *J. Phys.: Condens. Matter* **2002**, *14*, R703.

(5) Busch, S.; Smuda, C.; Pardo, L. C.; Unruh, T. Molecular mechanism of long-range diffusion in phospholipid membranes studied by quasielastic neutron scattering. *J. Am. Chem. Soc.* **2010**, *132*, 3232−3233.

(6) Armstrong, C. L.; Barrett, M. A.; Hiess, A.; Salditt, T.; Katsaras, J.; Shi, A.-C.; Rheinstädter, M. C. Effect of cholesterol on the lateral nanoscale dynamics of fluid membranes. *Eur. Biophys. J.* **2012**, *41*, 901−913.

(7) Armstrong, C. L.; Barrett, M. A.; Toppozini, L.; Kucerka, N.; Yamani, Z.; Katsaras, J.; Fragneto, G.; Rheinstadter, M. C. Co-existence of gel and fluid lipid domains in single-component phospholipid membranes. *Soft Matter* **2012**, *8*, 4687−4694.

(8) Armstrong, C. L.; Haüßler, W.; Seydel, T.; Katsaras, J.; Rheinstadter, M. C. Nanosecond lipid dynamics in membranes containing cholesterol. *Soft Matter* **2014**, *10*, 2600−2611.

(9) Schutz, G. J.; Schindler, H.; Schmidt, T. Single-molecule microscopy on model membranes reveals anomalous diffusion. *Biophys. J.* **1997**, *73*, 1073−1080.

(10) Clausen, M. P.; Lagerholm, B. C. Visualization of plasma membrane compartmentalization by high-speed quantum dot tracking. *Nano Lett.* **2013**, *13*, 2332−2337.

(11) Dadashvand, N.; Williams, L. A.; Othon, C. M. Heterogeneous rotational diffusion of a fluorescent probe in lipid monolayers. *Struct. Dyn.* **2014**, *1*, 054701.

(12) Murtola, T.; Róg, T.; Falck, E.; Karttunen, M.; Vattulainen, I. Transient ordered domains in single-component phospholipid bilayers. *Phys. Rev. Lett.* **2006**, *97*, 238102.

(13) Falck, E.; Róg, T.; Karttunen, M.; Vattulainen, I. Lateral diffusion in lipid membranes through collective flows. *J. Am. Chem. Soc.* **2008**, *130*, 44−45.

(14) Roark, M.; Feller, S. E. Molecular dynamics simulation study of correlated motions in phospholipid bilayer membranes. *J. Phys. Chem. B* **2009**, *113*, 13229−13234.

(15) Apajalahti, T.; Niemelä, P.; Govindan, P. N.; Miettinen, M. S.; Salonen, E.; Marrink, S.-J.; Vattulainen, I. Concerted diffusion of lipids in raft-like membranes. *Faraday Discuss.* **2010**, *144*, 411−430.

(16) Brandt, E. G.; Edholm, O. Stretched exponential dynamics in lipid bilayer simulations. *J. Chem. Phys.* **2010**, *133*, 115101.

(17) Javanainen, M.; Monticelli, L.; de la Serna, J. B.; Vattulainen, I. Free volume theory applied to lateral diffusion in langmuir monolayers: atomistic simulations for a protein-free model of lung surfactant. *Langmuir* **2010**, *26*, 15436−15444.

(18) Starr, F. W.; Hartmann, B.; Douglas, J. F. Dynamical clustering and a mechanism for raft-like structures in a model lipid membrane. *Soft Matter* **2014**, *10*, 3036−3047.

(19) Ghosh, R. N.; Webb, W. Automated detection and tracking of individual and clustered cell surface low density lipoprotein receptor molecules. *Biophys. J.* **1994**, *66*, 1301−1318.

(20) Kusumi, A.; Fujiwara, T. K.; Morone, N.; Yoshida, K. J.; Chadda, R.; Xie, M.; Kasai, R. S.; Suzuki, K. G. Membrane mechanisms for signal transduction: The coupling of the meso-scale raft domains to membrane-skeleton-induced compartments and dynamic protein complexes. *Semin. Cell Dev. Biol.* **2012**, *23*, 126−144.

(21) Miller, K. W.; Pang, K.-Y. Y. General anaesthetics can selectively perturb lipid bilayer membranes. *Nature* **1976**, *263*, 253−255.

(22) Woodson, P. B.; Traynor, M. E.; Schlapfer, W. T.; Barondes, S. H. Increased membrane fluidity implicated in acceleration of decay of post-tetanic potentiation by alcohols. *Nature* **1976**, *260*, 797−799.

(23) Curran, M.; Seeman, P. Alcohol tolerance in a cholinergic nerve terminal: relation to the membrane expansion-fluidization theory of ethanol action. *Science* **1977**, *197*, 910−911.

(24) Stephens, C. L.; Shinitzky, M. Modulation of electrical activity in Aplysia neurones by cholesterol. *Nature* **1977**, *270*, 267−268.

(25) Cotterill, R. Does the nerve action potential involve a localized phase transition of the lipid bilayer? *Phys. Scr.* **1980**, *22*, 188.

DOI: 10.1021/acs.jpcb.6b02982
J. Phys. Chem. B 2016, 120, 5172−5182

(26) Koster, K.; Lei, Y.; Anderson, M.; Bryant, G. Effects of vitrified and nonvitrified sugars on phosphatidylcholine fluid-to-gel phase transitions. *Biophys. J.* **2000**, *78*, 1932−1946.
(27) Seeger, H.; Gudmundsson, M.; Heimburg, T. How anesthetics, neurotransmitters, and antibiotics influence the relaxation processes in lipid membranes. *J. Phys. Chem. B* **2007**, *111*, 13858−13866.
(28) Xie, A. F.; Yamada, R.; Gewirth, A. A.; Granick, S. Materials science of the gel to fluid phase transition in a supported phospholipid bilayer. *Phys. Rev. Lett.* **2002**, *89*, 246103.
(29) Zhang, L.; Granick, S. Dynamical heterogeneity in supported bilayers. *MRS Bull.* **2006**, *31*, 527−531.
(30) Berthier, L. Dynamic heterogeneity in amorphous materials. *Physics* **2011**, *4*, 42.
(31) Starr, F. W.; Douglas, J. F.; Sastry, S. The relationship of dynamical heterogeneity to the Adam-Gibbs and random first-order transition theories of glass formation. *J. Chem. Phys.* **2013**, *138*, 12A541.
(32) Almeida, P. F.; Vaz, W. L.; Thompson, T. Lateral diffusion in the liquid phases of dimyristoylphosphatidylcholine/cholesterol lipid bilayers: a free volume analysis. *Biochemistry* **1992**, *31*, 6739−6747.
(33) Almeida, P. F.; Vaz, W. L.; Thompson, T. Lipid diffusion, free area, and molecular dynamics simulations. *Biophys. J.* **2005**, *88*, 4434−4438.
(34) Lindblom, G.; Orädd, G. Lipid lateral diffusion and membrane heterogeneity. *Biochim. Biophys. Acta, Biomembr.* **2009**, *1788*, 234−244.
(35) Cooke, I. R.; Deserno, M. Solvent-free model for self-assembling fluid bilayer membranes: Stabilization of the fluid phase based on broad attractive tail potentials. *J. Chem. Phys.* **2005**, *123*, 224710.
(36) Marrink, S. J.; Risselada, H. J.; Yefimov, S.; Tieleman, D. P.; de Vries, A. H. The MARTINI force field: coarse grained model for biomolecular simulations. *J. Phys. Chem. B* **2007**, *111*, 7812−7824.
(37) Kučerka, N.; Tristram-Nagle, S.; Nagle, J. F. Closer look at structure of fully hydrated fluid phase DPPC bilayers. *Biophys. J.* **2006**, *90*, L83−L85.
(38) Ballew, R. M.; Sabelko, J.; Gruebele, M. Observation of distinct nanosecond and microsecond protein folding events. *Nat. Struct. Biol.* **1996**, *3*, 923−926.
(39) Simons, K.; Toomre, D. Lipid rafts and signal transduction. *Nat. Rev. Mol. Cell Biol.* **2000**, *1*, 31−39.
(40) Marrink, S. J.; Risselada, J.; Mark, A. E. Simulation of gel phase formation and melting in lipid bilayers using a coarse grained model. *Chem. Phys. Lipids* **2005**, *135*, 223−244.
(41) Duncan, S. L.; Larson, R. G. Comparing experimental and simulated pressure-area isotherms for DPPC. *Biophys. J.* **2008**, *94*, 2965−2986.
(42) Duncan, S. L.; Dalal, I. S.; Larson, R. G. Molecular dynamics simulation of phase transitions in model lung surfactant monolayers. *Biochim. Biophys. Acta, Biomembr.* **2011**, *1808*, 2450−2465.
(43) Van Der Spoel, D.; Lindahl, E.; Hess, B.; Groenhof, G.; Mark, A. E.; Berendsen, H. J. C. GROMACS: fast, flexible, and free. *J. Comput. Chem.* **2005**, *26*, 1701−1718.
(44) Lis, M.; Wizert, A.; Przybylo, M.; Langner, M.; Swiatek, J.; Jungwirth, P.; Cwiklik, L. The effect of lipid oxidation on the water permeability of phospholipids bilayers. *Phys. Chem. Chem. Phys.* **2011**, *13*, 17555−17563.
(45) Janiak, M. J.; Small, D. M.; Shipley, G. G. Temperature and compositional dependence of the structure of hydrated dimyristoyl lecithin. *J. Biol. Chem.* **1979**, *254*, 6068−6078.
(46) Tristram-Nagle, S.; Nagle, J. F. Lipid bilayers: thermodynamics, structure, fluctuations, and interactions. *Chem. Phys. Lipids* **2004**, *127*, 3−14.
(47) Tenchov, B. On the reversibility of the phase transitions in lipid-water systems. *Chem. Phys. Lipids* **1991**, *57*, 165−177.
(48) Katsaras, J.; Yang, D. S.; Epand, R. M. Fatty-acid chain tilt angles and directions in dipalmitoyl phosphatidylcholine bilayers. *Biophys. J.* **1992**, *63*, 1170−5.
(49) Hub, J. S.; Salditt, T.; Rheinstadter, M. C.; de Groot, B. L. Short-range order and collective dynamics of DMPC bilayers: a comparison between molecular dynamics simulations, X-ray, and neutron scattering experiments. *Biophys. J.* **2007**, *93*, 3156−3168.
(50) Bernard, E. P.; Krauth, W. Two-step melting in two dimensions: first-order liquid-hexatic transition. *Phys. Rev. Lett.* **2011**, *107*, 155704.
(51) Smith, G. S.; Sirota, E. B.; Safinya, C. R.; Plano, R. J.; Clark, N. A. X-ray structural studies of freely suspended ordered hydrated DMPC multimembrane films. *J. Chem. Phys.* **1990**, *92*, 4519.
(52) Jeon, J.-H.; Monne, H. M.-S.; Javanainen, M.; Metzler, R. Anomalous diffusion of phospholipids and cholesterols in a lipid bilayer and its origins. *Phys. Rev. Lett.* **2012**, *109*, 188103.
(53) Ehrig, J.; Petrov, E. P.; Schwille, P. Near-critical fluctuations and cytoskeleton-assisted phase separation lead to subdiffusion in cell membranes. *Biophys. J.* **2011**, *100*, 80−9.
(54) Javanainen, M.; Hammaren, H.; Monticelli, L.; Jeon, J.-H.; Miettinen, M. S.; Martinez-Seara, H.; Metzler, R.; Vattulainen, I. Anomalous and normal diffusion of proteins and lipids in crowded lipid membranes. *Faraday Discuss.* **2013**, *161*, 397−417.
(55) Niemelä, P. S.; Miettinen, M. S.; Monticelli, L.; Hammaren, H.; Bjelkmar, P.; Murtola, T.; Lindahl, E.; Vattulainen, I. Membrane proteins diffuse as dynamic complexes with lipids. *J. Am. Chem. Soc.* **2010**, *132*, 7574−7575.
(56) Kneller, G. R.; Baczynski, K.; Pasenkiewicz-Gierula, M. Communication: consistent picture of lateral subdiffusion in lipid bilayers: molecular dynamics simulation and exact results. *J. Chem. Phys.* **2011**, *135*, 141105.
(57) Forrey, C.; Saylor, D. M.; Silverstein, J. S.; Douglas, J. F.; Davis, E. M.; Elabd, Y. A. Prediction and validation of diffusion coefficients in a model drug delivery system using microsecond atomistic molecular dynamics simulation and vapour sorption analysis. *Soft Matter* **2014**, *10*, 7480−7494.
(58) Scomparin, C.; Lecuyer, S.; Ferreira, M.; Charitat, T.; Tinland, B. Diffusion in supported lipid bilayers: influence of substrate and preparation technique on the internal dynamics. *Eur. Phys. J. E: Soft Matter Biol. Phys.* **2009**, *28*, 211−220.
(59) Hansen, J. P.; McDonald, I. R. *Theory of Simple Liquids*; Academic Press: London, 1986.
(60) Chaudhuri, P.; Berthier, L.; Kob, W. Universal nature of particle displacements close to glass and jamming transitions. *Phys. Rev. Lett.* **2007**, *99*, 060604.
(61) Zhang, H.; Khalkhali, M.; Liu, Q.; Douglas, J. F. String-like cooperative motion in homogeneous melting. *J. Chem. Phys.* **2013**, *138*, 12A538.
(62) Jin, A. J.; Edidin, M.; Nossal, R.; Gershfeld, N. L. A singular state of membrane lipids at cell growth temperatures. *Biochemistry* **1999**, *38*, 13275−13278.
(63) Stauffer, D.; Aharony, A. *Introduction to Percolation Theory*; Taylor and Francis: London, 1998.
(64) Steinhardt, P. J.; Nelson, D. R.; Ronchetti, M. Bond-orientational order in liquids and glasses. *Phys. Rev. B: Condens. Matter Mater. Phys.* **1983**, *28*, 784−805.
(65) Starr, F. W.; Sastry, S.; Douglas, J. F.; Glotzer, S. C. What do we learn from the local geometry of glass-forming liquids. *Phys. Rev. Lett.* **2002**, *89*, 125501.
(66) Sciortino, F.; Geiger, A.; Stanley, H. E. Network defects and molecular mobility in liquid water. *J. Chem. Phys.* **1992**, *96*, 3857.
(67) Giovambattista, N.; Buldyrev, S. V.; Starr, F. W.; Stanley, H. E. Clusters of mobile molecules in supercooled water. *Phys. Rev. E* **2005**, *72*, 011202.
(68) Donati, C.; Glotzer, S. C.; Poole, P. H.; Kob, W.; Plimpton, S. J. Spatial correlations of mobility and immobility in a glass-forming Lennard-Jones liquid. *Phys. Rev. E* **1999**, *60*, 3107−3119.
(69) Angelini, T. E.; Hannezo, E.; Trepat, X.; Marquez, M.; Fredberg, J. J.; Weitz, D. A. Glass-like dynamics of collective cell migration. *Proc. Natl. Acad. Sci. U. S. A.* **2011**, *108*, 4714−4719.
(70) Sadati, M.; Nourhani, A.; Fredberg, J. J.; Taheri Qazvini, N. Glass-like dynamics in the cell and in cellular collectives. *Wiley Interdiscip. Rev. Syst. Biol. Med.* **2014**, *6*, 137−149.

DOI: 10.1021/acs.jpcb.6b02982
J. Phys. Chem. B 2016, 120, 5172−5182